

## A plasmonic turn-on insulin sensing platform on centimeter scale nanostructure arrays

Thanh Thi Van Nguyen

School of Materials Science and Engineering, Hanoi University of Science and Technology, Hanoi, Vietnam

[thanh.nguyenthivan@hust.edu.vn](mailto:thanh.nguyenthivan@hust.edu.vn)

**ABSTRACT** We present a plasmonic turn-on biosensing assay for insulin detection via aptamer DNA based on the plasmonic interaction of centimeter scale gold/silver double-layer nanodisk arrays and gold nanoparticles. The large-scale nanostructures were fabricated by laser interference lithography technique. The detecting optical signal-extinction spectra of the system were monitored by UV-visible spectrophotometry. The 3D finite-difference time-domain simulation was used to observe the plasmonic interaction of the sensing system. The platform exhibits an exceptionally large turn-on signal by a 120 nm red shift of the localized surface plasmonic resonance peak, results in the limit detection of 140 pM. The centimeter-scale localized surface plasmon resonance nanostructures combined with turn-on design scheme would offer a promising sensor-on-chip biosensing platform.

**KEYWORDS** insulin sensing, localized surface plasmon, plasmonic interaction, nanostructure

**ACKNOWLEDGEMENTS** This research is funded by Hanoi University of Science and Technology (HUST) under project number T2022-PC-083.

**FOR CITATION** Thanh Thi Van Nguyen A plasmonic turn-on insulin sensing platform on centimeter scale nanostructure arrays. *Nanosystems: Phys. Chem. Math.*, 2024, **15** (2), 300–306.

### 1. Introduction

Diabetes can lead to many dangerous complications therefore necessary to detect it early so that effective treatments can be intervened in the early stages [1]. Type 1 diabetes is related to the insulin deficiency leads to glucose in the blood not being absorbed [2]. Detection of insulin is critical for diagnosis of this high risk disease [3]. Conventional methods applied for insulin sensing include immunoassay methods (RIA – Radioimmunoassay [4], ELISA – Enzyme-Linked Immunosorbent Assay [5], and CLIA chemiluminescence immunoassay [6]), analytical chemistry methods (fluorescent detection [7], mass spectrometry [8], Raman spectroscopy [9]), electrochemical spectrometry [10]. These methods have their own advantages and some limitations needed to improve including selectivity, detection time, multiplex sample preparation, electronic signal reading instrumentation, and complex signal enhancement procedure [11].

Recently, the usage of localized surface plasmon resonance of nanostructures in biological sensing assays has become a promising method due to its distinctive characteristics. Localized surface plasmon resonance (LSPR) is widely known as the collective charge oscillations that arises around nanoscale structures when light is illuminated onto the surface [12]. LSPR owns highly sensitivity to the localized refractive index (RI) changes. The biomolecular attachment on the surface of the nanostructures changes the local RI in the vicinity of the sensing surface that results in a sensitive response in LSPR-induced light absorption spectrum which is used to conduct specific detection [13]. LSPR – based detection by using nanoscale structures fabricated in a large – scale area has been demonstrated to be an effective platform for biosensing offers the advantage of being easily multiplexed to enable high throughput screening in an array format [14–20].

Laser interference lithography (LIL) is one of the simple techniques to produce a large area of well ordering arrays of LSPR nanostructures [21, 22]. In addition, this technique can be used to fabricate the nanostructures array in all available rigid or flexible substrates. With one shot of laser exposure in few minutes, by manipulating carefully the laser incident beam angles as well as the relative angles between exposure times, the size, shape can be altered flexibly [23]. Previously, we fabricated 2D gold/silver nanodisks by LIL with high refractive index sensitivity and successfully used these nanodisks for DNA sensing platform [19].

Nucleic acid aptamers have been widely used as chemical antibodies in various biological sensing due to the specific recognition and tight binding to their targets [24, 25]. The insulin aptamers are single stranded DNAs containing a two-repeat sequence of the insulin-linked polymorphic region (ILPR) of the human insulin gene promoter region [26, 27]. They can fold into G-quadruplex oligonucleotides in the presence of insulin with high specificity and affinity. Many research groups have used insulin aptamers as ligands in insulin detection [28–31].

In this work, we report the experimental assay for insulin sensing with a turn-on design sensing scheme by using fabricated 2D gold/silver nanodisks, gold nanoparticles and insulin aptamers. Our objective is to integrate the high sensitivity resulting from the plasmonic interactions between gold nanoparticles and large-scale gold/silver nanodisk array and the high selectivity resulting from the specific binding of the insulin to their aptamers. The “turn-on” design means

that the lesser insulin concentration presents the higher optical signal of plasmonic system can be generated, consequently, the higher sensitivity can be achieved.

## 2. Detection scheme and working principle

The detection scheme is shown in Fig. 1. The detecting optical signal in this design is LSPR peak shift of the 2D gold/silver nanodisks as the gold nanoparticles are attached to the nanodisk surfaces by insulin aptamer DNA. The aptamer DNA was complementary with two different single DNA strands attached to 2D gold/silver double-layer nanodisks (capture DNA c1) and gold nanoparticles (capture DNA c2). Without the presence of insulin, the aptamers link the gold nanoparticles to the nanodisk surfaces and cause the LSPR peak shift (signal on). Since the binding affinity of insulin to insulin aptamer DNA to form G-quadruplex is much higher than that to complementary single DNA strands, the insulin aptamers have prior bindings to insulin rather than to their complementary strands. Therefore, once the insulin is introduced there is lesser available insulin aptamer DNA for attachment of gold nanoparticles to the nanodisk surfaces. As a result, smaller LSPR peak shifts of the 2D gold/silver nanodisks are generated (signal off). The presence of various concentrations of insulin in the system will modulate the attachment of gold nanoparticles due to the interaction of insulin and their aptamer, hence, insulin can be detected by the corresponding LSPR peak shift of the nanodisks. By observing the LSPR spectrum of the 2D gold/silver nanodisks, insulin could be detected selectively and sensitively.

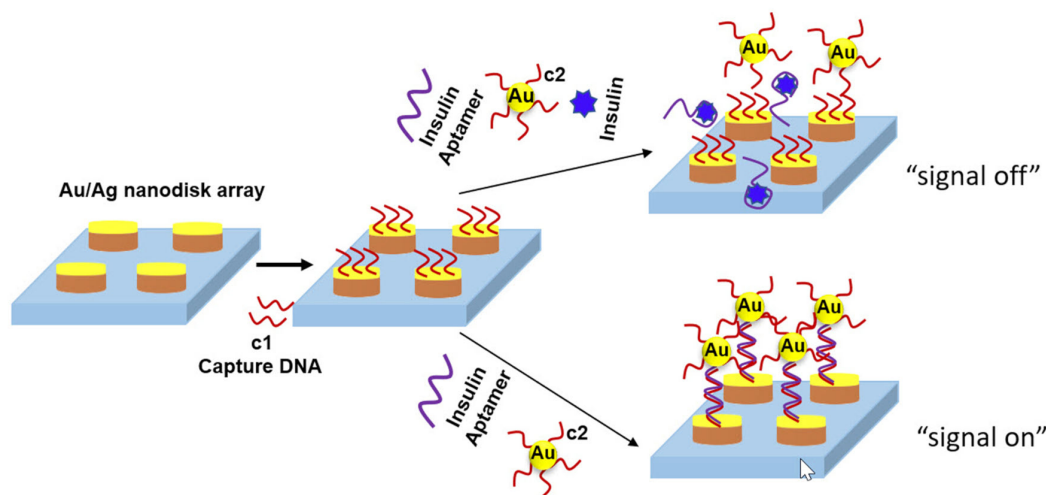


FIG. 1. "Turn on" insulin detection scheme

The gold nanoparticles in this design are sensing indicators as well as the plasmonic signal amplifying agents. Once they are brought closely enough to the nanodisk surfaces, the plasmonic interaction between them occurs [32]. As a result, the electromagnetic field surrounding them increases, the sensitivity to the localized refractive index (RI) changes of the nanodisks enhances significantly. Therefore, the lesser biological binding events on the nanodisk surfaces still cause a large LSPR peak shift for the detection.

The key point of our detection design is turn-on strategy. With the same concentration of insulin aptamer DNA introduced, the lower insulin concentration is needed to detect in the system, the more insulin aptamer DNA are left, the more gold nanoparticles are attached to the nanodisk surface, and the larger LSPR peak shift is recorded. By that turn-on principle, the detecting signal is enlarged as the concentration of the sensing agent is lessened. Hence, the lower concentration of sensing agent could be detected.

## 3. Materials and methods

### 3.1. Materials

All substrates (silicon, quartz, PEN) were bought from Photonik Pte Ltd (Singapore). The photoresist maN1407 and maR404 remover used for laser interference lithography was brought from Micro resist technology (Germany). The metallic materials used for fabrication of nanodisks (chromium, silver, gold) were supplied by MOS Group Pte Ltd (Singapore). The chemicals, insulin and DNA strands used in this study were bought from Sigma Aldrich (Singapore). The DNA sequences are shown in Table 1.

TABLE 1. DNA sequences

Name	Sequences
C1-Capture DNA	3'-ACCATCCCACAGAAGTTT [thiolC6]-5'
C2-Capture DNA	3'-[thiolC3] TTTCCACCACCCCCCCA-5'
IA-Aptamer DNA	5'-GGTGGTGGGGGGGGTTGGTAGGGGTGTC TTCTT-3'

### 3.2. Fabrication of 2D gold/silver double-layer nanodisks on centimeter scale substrate

All 2D gold/silver double-layer nanodisks used in this study were fabricated by laser interference lithography (LIL) technique in a homebuilt *Lloyd's-mirror* LIL system with a 325 nm He–Cd laser. The procedure was similar to the standard lithography procedure and described in our previous study in detail [19]. Shortly, the negative photoresist firstly coated on the substrates, then they were exposed to laser on the LIL system to create holes array. After that, the 20 nm thick silver layer and 10 nm thick gold layer were deposited by an electron-beam evaporator to form 30 nm thick gold/silver nanodisk arrays after lift-off process.

### 3.3. Capture DNA attachment to gold/silver nanodisks and gold nanoparticles

Gold nanoparticles ( $\sim 15$  nm) were synthesized by citrate reduction of HAuCl<sub>4</sub> method [33]. Capture DNA attachment to gold/silver nanodisks and gold nanoparticles were followed by the same procedure as were described in our previous study [19]. In brief, two types of capture DNA strands (Table 1) were used, the capture strand  $c_1$  was attached to gold/silver nanodisks and the capture strand  $c_2$  was attached to gold nanoparticles. These 3'- or 5'-terminal disulfide groups of single-stranded capture DNAs were first cleaved by immersing these DNA strands in a mixture of 0.1 M dithiothreitol (DTT) and phosphate buffer solution (pH = 8.0) for 2 hours, afterwards purified on NAP-5 columns (GE Healthcare). Then the corresponding purified capture DNA solution was brought to 15 nm gold nanoparticles and the gold/silver nanodisks for attachment. Finally, the rinsing process was carried out to remove the non-binding capture DNAs.

### 3.4. Insulin sensing experiment

At first, the attachment of capture DNA to the nanodisk arrays and gold nanoparticles was performed. Then, 1  $\mu$ M insulin aptamer DNA (IA) in insulin buffer (50 mM Tris-HCl, 10 mM KCl, 100 mM NaCl, pH = 8.0) was subject to the heating process to unfold the DNA sequences to increase the binding affinity of the aptamer to insulin. The heating process was carried out at 90 °C in 10 minutes and then the aptamer solution was cooled in 30 minutes to room temperature. After that, the insulin was introduced to the aptamer solution then allowed to incubate at room temperature in 1 hour. The sensing concentration of insulin ranged from 10 pM to 50  $\mu$ M. For the experiment with no insulin introduction, this step was skipped. Next, DNA-captured gold nanoparticles were added to the incubated mixture of insulin and their aptamers. After that, this final mixture was brought to the DNA-capture gold/silver nanodisk arrays. It was allowed to incubate in 2 hours then rinsed with insulin buffer thoroughly. Finally, the modified gold/silver nanodisk arrays were brought to the measurement step to obtain the extinction spectra. In the selectivity experiments, the same procedure was carried out with other proteins (bovine serum albumin (BSA), and alkaline phosphatase (ALP) and thrombin).

### 3.5. Characterization

To observe the morphology of nanodisks and the attachment of gold nanoparticles to the nanodisk surface, a scanning electron microscope (SEM) was used (NOVA NanoSEM 230-FEI, USA). The extinction spectra of the nanodisks were characterized by a UV-1800 UV-VISspectrophotometer (Shimadzu, Japan) in transmission mode.

## 4. Result and discussion

### 4.1. Observation of 2D gold/silver nanodisks

After fabrication, the 2D Au/Ag nanodisks were observed by SEM to confirm the size of the nanostructures. The diameter of the disks is 330 nm approximately. The size of the disk can be altered by changing the interference angle of LIL system. This is the smallest size of the disks that can be fabricated by our home-made LIL system. The nanodisks are double layer, the 20 nm thick silver layers are underneath and 10 nm thick gold layers are on the top. The double layer was fabricated to take advantage of the high refractive index sensing of silver and the biological compatibility of gold. The centimeter scale of nanodisks was obtained by one shot of laser exposure by LIL technique on many types of substrates. As shown in Figs. 2b and 2c, the nanodisks were fabricated on silicon, quartz and polyethylene naphthalate (PEN) substrates. In this study, all samples were fabricated on quartz substrate to get high transmittance for optical signal detection.

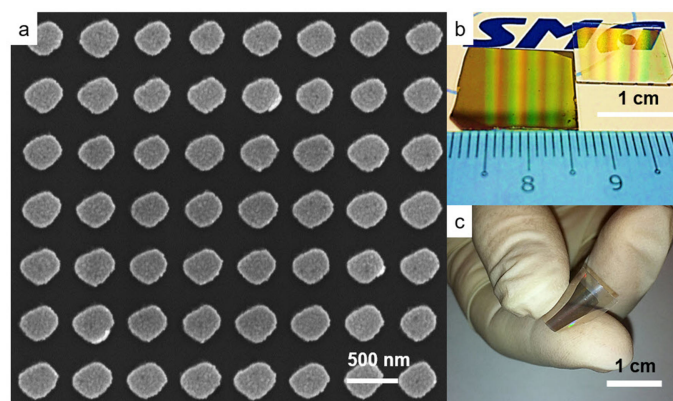


FIG. 2. Fabricated 2D gold/silver nanodisks: (a) SEM image, (b) centimeter scale of nanodisks on rigid substrate (quartz, silicon) and (c) flexible substrate (PEN)

#### 4.2. Viability and selectivity of the detection scheme

To examine the viability of the detection scheme, the LSPR peak shifts of two experiments with and without insulin introduction were recorded and shown in Figs. 3a and 3b, respectively. Consideration of 1:1 binding ratio of insulin and their aptamer,  $5 \mu\text{M}$  insulin and  $1 \mu\text{M}$  aptamer was introduced in the experiments to eliminate the free aptamer (as described in 3.4). The LSPR peak shift of the nanodisks in this experiment was 50 nm (Fig. 3a) while the LSPR peak shift of the nanodisks in insulin absence experiment was 120 nm (Fig. 3b). The LSPR peak shift of the nanodisks in these experiments results from the changing in local refractive index at the surface of the nanodisks where insulin aptamer and gold nanoparticles were attached. No insulin was introduced, there were more DNA aptamers which are linkers attaching more gold nanoparticles to nanodisk surfaces. Consequently, the larger change in local refractive index was caused and the larger LSPR peak shifts were obtained. These recorded values proved that the “turn on” strategy detection worked successfully.

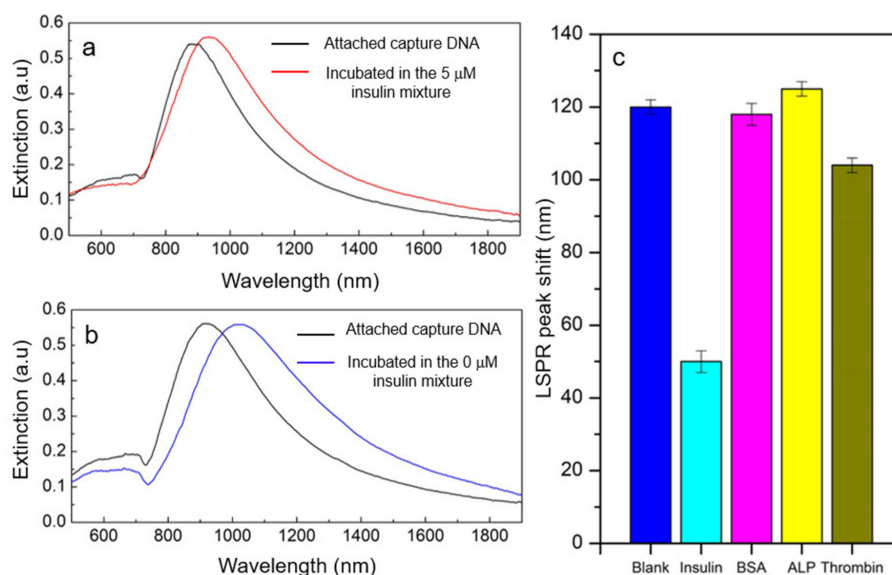


FIG. 3. LSPR peak shifts of viability and selectivity experiments with  $1 \mu\text{M}$  of insulin aptamer DNA: a – in presence of  $5 \mu\text{M}$  insulin, b – in absence of insulin (blank sample), c – in presence of  $5 \mu\text{M}$  BSA, ALP and thrombin respectively

To validate the selectivity of the design, the same experiment was carried out with the  $1 \mu\text{M}$  insulin aptamer and  $5 \mu\text{M}$  of three different proteins: bovine serum albumin (BSA), and alkaline phosphatase (ALP) and thrombin. The recorded LSPR peak shifts of the nanodisks in these experiments were shown in Fig. 3c. The LSPR peak shifts of experiments with BSA, ALP and thrombin were 118 nm, 125 and 104 nm, respectively. These values are in the order of the peak shift of the blank sample (the sample without insulin) and distinctly higher than that of the sample with insulin. This means that the detection design exclusively “turn off” with insulin presence. These results obviously demonstrated the high selectivity of our insulin detection platform.

### 4.3. Signal enhancement by plasmonic interactions

Signal enhancement is the key to lower the limit of detection of molecules under consideration. The LSPR based sensing works on monitoring the LSPR peak shift according to the local refractive index change of the LSPR nanostructures. Without amplification agents, the DNA strands binding events on the LSPR nanostructure surface usually cause small changes in RI and results in low sensitivity of the detection [32, 34]. As mentioned, the gold nanoparticles in our detection played as signal enhanced agents by taking advantage of plasmonic interactions between gold/silver nanodisks and gold nanoparticles. The plasmonic interactions between them were verified by using the finite difference time domain (FDTD) simulation as shown in Figs. 4a and 4b. The simulated distance between the nanodisk and the gold nanoparticle is equal to the length of the linker insulin aptamer (the length of 32 bases strand is approximately 10 nm). As can be seen, with presence of the gold nanoparticle close to the nanodisk surface, the plasmon interaction between them makes the electromagnetic field of the nanodisk increases significantly. It should be emphasized that, during the sensing experiments there were many gold nanoparticles brought to the nanodisk surfaces as presented in the corresponding SEM image in Figs. 4c and 4d. In addition, the 2D gold/silver nanodisks were in a centimeter scale. Due to these factors, the collective resonance electromagnetic field of nanodisks in the sensing platform was extremely enhanced and resulting in an incredibly LSPR peak shifts that was caused by the binding of DNA to the nanodisk surfaces. In our “turn-on” insulin detection design, this enhancement strategy is greatly effective since the lesser insulin was introduced, the larger LSPR peak shift was created.

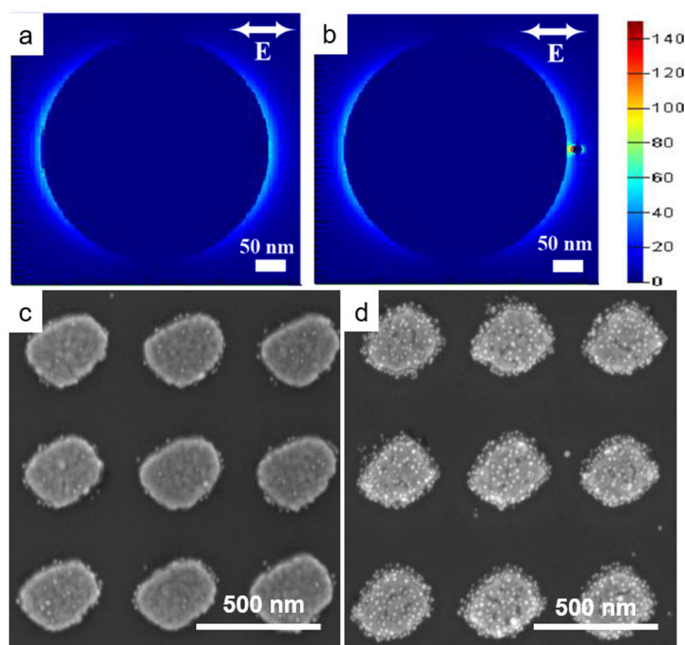


FIG. 4. Plasmonic interaction between gold nanoparticles and gold/silver nanodisks: (a) simulated electromagnetic field of one gold/silver nanodisk, (b) simulated electromagnetic field enhancement between one gold nanoparticle and one gold/silver nanodisk; attachment of gold nanoparticle to 2D gold/silver nanodisks (c) in the absence of insulin (blank sample) and (d) in the presence of  $5 \mu\text{M}$  insulin

However, the unexpected of free DNA aptamer bindings were also enhanced. There were a number of nanoparticles bound on the nanodisk surfaces (Fig. 4c) and they caused a measurable LSPR peak shift of the system (Fig. 3a) in the experiment with insulin introduction. This evidence proposed that there was an amount of free insulin aptamer that did not bind to insulin in spite of the concentration of insulin ( $5 \mu\text{M}$ ) is five times higher than that of their aptamer DNA ( $1 \mu\text{M}$ ). These results may be caused by the dynamic range of the biological interaction between insulin and their aptamer [34]. Nevertheless, the affection of the inactive insulin aptamer binding was diminished in our “turn-on” detection scheme.

### 4.4. Sensitivity and specificity

The sensitivity of the insulin detection platform was demonstrated by a series of experiments at various concentrations from  $10 \text{ pM}$  to  $50 \mu\text{M}$  of insulin in the presence of the same concentration of aptamer DNA ( $1 \mu\text{M}$ ). The LSPR peak shifts of the system in these experiments are presented in Fig. 5a. Obviously, as the concentration of insulin decreases from  $50 \mu\text{M}$  to  $10 \text{ pM}$ , the value of LSPR peak shift increases from  $44 \text{ nm}$  to  $117 \text{ nm}$ . The combination of the “turn-on” strategy with plasmonic enhancement over a centimeter scale of our system produces a distinctive shift ( $117 \text{ nm}$ ) of the LSPR peak with a small amount of insulin introduction ( $10 \text{ pM}$ ). To the best of our knowledge, such a large shift of the extinction spectrum peak has not been reported in literature of LSPR based insulin sensing, till date. We used the ICH

technique to calculate the limit of detection (LOD) of our sensing assay [35],  $\text{LOD} = 3.3\sigma/s$  ( $\sigma$  – standard deviation of response,  $s$  – slope of the calibration curve). The data of the LSPR peak shifts in the insulin concentration range of 0 M to 500 pM were used to compute the LOD (the inset of Fig. 4). The calculated LOD of our insulin detection platform was 140 pM. The LOD of our sensing system is comparable to the concentration of free insulin in the blood, blood plasma or interstitial fluid that is in the picomolar range [11]. The result asserts strongly that our unoptimized system works on insulin detection with high sensitivity.

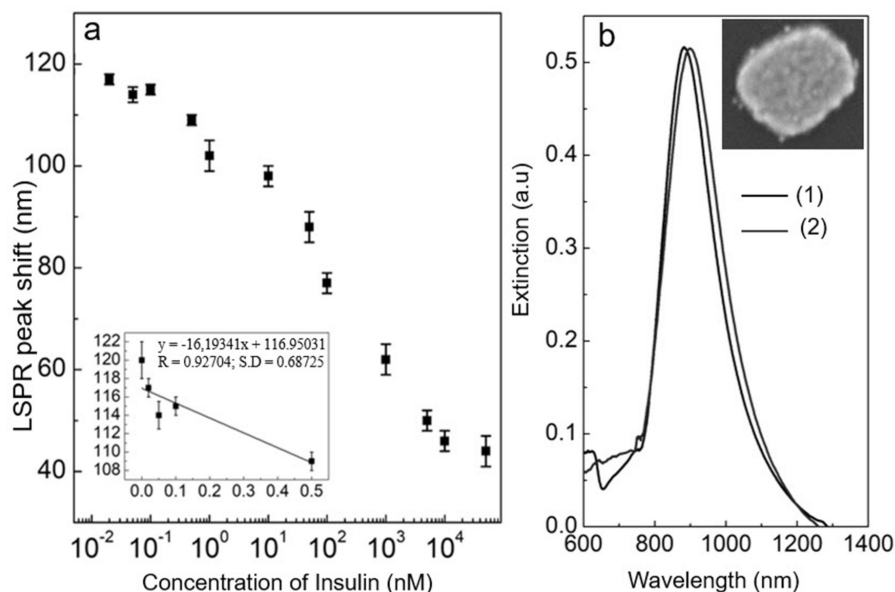


FIG. 5. Sensitivity and specificity experimental results: (a) LSPR peak shifts of 2D gold/silver nanodisks after the incubation with various concentrations of insulin, (b) LSPR peak shifts of 2D gold/silver nanodisks after the incubation with 5  $\mu\text{M}$  insulin, DNA-captured gold nanoparticles, 1  $\mu\text{M}$  adenosine aptamer DNA (1 – after attaching capture DNA, 2 – after the incubation)

The nonspecific binding experiments were carried out further to confirm the specificity of the sensing system. All biological components of the system were observed the nonspecific interaction to the nanodisks. Fig. 5b shows the LSPR peak shift of nanodisk after incubating with insulin, DNA-captured gold nanoparticles, adenosine aptamer (single DNA strands have the same base number as insulin aptamers but they form the G-quadruplex with adenosine not insulin). The nonspecific interactions of these components with the nanodisks only results in 15 nm red shift of the nanodisk LSPR peak. The SEM image inset also showed a couple of gold nanoparticles attached to the nanodisk surface after the nonspecific incubation. These data proved that the LSPR peak shifts in our sensing experiments were predominantly attributed to specific biological binding.

## 5. Conclusion

In summary, we reported a “turn-on” plasmon insulin detection platform by using LSPR structures combined with plasmonic amplification as optical transducers. The LSPR structures in this study were Au/Ag nanodisks of 320 nm diameter that were fabricated into centimeter scale 2D arrays on quartz substrates by laser interference lithography. The “turn on” detection strategy helped one to maximize the detecting optical signals at low concentrations of detecting insulin and to eliminate the nonspecific biological interactions. The plasmonic amplification is contributed by localized plasmonic interactions between a huge number of 15 nm gold nanoparticles with Au/Ag nanodisks. The combination of these factors led to the high sensitivity of our detection system that achieved the LOD of 140 pM that is comparable as picomolar range of insulin level in human body. The specificity of the system is assured by the distinct biological interaction of insulin and their DNA aptamers during the detection. The principles of our sensing platform can be applied for other DNA aptamer linked biological agents even small molecules. In addition, the large area of the fabricated LSPR nanostructures on all type of substrates in a short time may be an alternative approach for the lab-on-chip biological sensing.

## References

- [1] Morris A. New test for diabetes insipidus. *Nature Reviews Endocrinology*, 2019, **15** (10), P. 564–565.
- [2] Mane K., Chaluvaraju K., Niranjan M., Zaranappa T., Manjuthaj T. Review of Insulin and its Analogues in Diabetes Mellitus. *J. of basic and clinical pharmacy*, 2012, **3**, P. 283–293.

- [3] Lian K., Feng H., Liu S., Wang K., Liu Q., Deng L., Wang G., Chen Y., Liu G. Insulin quantification towards early diagnosis of prediabetes/diabetes. *Biosensors and Bioelectronics*, 2022, **203**, 114029.
- [4] Warnken T., Huber K., Feige K. Comparison of three different methods for the quantification of equine insulin. *BMC Veterinary Research*, 2016, **12** (1), 196.
- [5] Manley S.E., Stratton I.M., Clark P.M., Luzio S.D. Comparison of 11 Human Insulin Assays: Implications for Clinical Investigation and Research. *Clinical Chemistry*, 2007, **53** (5), P. 922–932.
- [6] Tanaka T., Matsunaga T. Fully Automated Chemiluminescence Immunoassay of Insulin Using Antibody-Protein A/Bacterial Magnetic Particle Complexes. *Analytical Chemistry*, 2000, **72** (15), P. 3518–3522.
- [7] Ho J.A., Zeng S., Huang M., Kuo H. Development of liposomal immunosensor for the measurement of insulin with femtomole detection. *Analytica Chimica Acta*, 2006, **556** (1), P. 127–132.
- [8] Gillette M.A., Carr S.A. Quantitative analysis of peptides and proteins in biomedicine by targeted mass spectrometry. *Nature Methods*, 2013, **10** (1), P. 28–34.
- [9] Cho H., Kumar S., Yang D., Vaidyanathan S., Woo K., Garcia I., Shue H.J., Yoon Y., Ferreri K., Choo H. Surface-Enhanced Raman Spectroscopy-Based Label-Free Insulin Detection at Physiological Concentrations for Analysis of Islet Performance. *ACS Sensors*, 2018, **3** (1), P. 65–71.
- [10] Kimmel D.W., LeBlanc G., Meschievitz M.E., Cliffel D.E. Electrochemical Sensors and Biosensors. *Analytical Chemistry*, 2012, **84** (2), P. 685–707.
- [11] Soffe R., Nock V., Chase J.G. Towards Point-of-Care Insulin Detection. *ACS Sensors*, 2019, **4** (1), P. 3–19.
- [12] Mayer K.M., Hafner J.H. Localized Surface Plasmon Resonance Sensors. *Chemical Reviews*, 2011, **111** (6), P. 3828–3857.
- [13] Takeshima N., Sugawa K., Noguchi M., Tahara H., Jin S., Takase K., Otsuki J., Tamada K. Synthesis of Ag Nanoprisms with Precisely-tuned Localized Surface Plasmon Wavelengths by Sequential Irradiation of Light of Two Different Wavelengths. *Chemistry Letter*, 2020, **49** (3), P. 240–243.
- [14] Luo X., Zhu C., Saito M., Espulgar W.V., Dou X., Terada Y., Obara A., Uchiyama S., Tamiya E. Cauliflower-Like Nanostructured Localized Surface Plasmon Resonance Biosensor Chip for Cytokine Detection. *Bulletin of the Chemical Society of Japan*, 2020, **93** (9), P. 1121–1126.
- [15] Ortega M.A., Rodríguez-Comas J., Yavas O., Velasco-Mallorquí F., Balaguer-Trias J., Parra V., Novials A., Servitja J.M., Quidant R., Ramón-Azcón J. In Situ LSPR Sensing of Secreted Insulin in Organ-on-Chip. *Biosensors*, 2021, **11** (5), 138.
- [16] Hammond J.L., Bhalla N., Rafiee S.D., Estrela P. Localized Surface Plasmon Resonance as a Biosensing Platform for Developing Countries. *Biosensors*, 2014, **4** (2), P. 172–188.
- [17] Maphanga C., Manoto S., Ombinda-Lemboumba S., Ismail Y., Mthunzi-Kufa P. Localized surface plasmon resonance biosensing of Mycobacterium tuberculosis biomarker for TB diagnosis. *Sensing and Bio-Sensing Research*, 2023, **39**, 100545.
- [18] Bonyár A. Label-Free Nucleic Acid Biosensing Using Nanomaterial-Based Localized Surface Plasmon Resonance Imaging: A Review. *ACS Applied Nano Materials*, 2020, **3** (9), P. 8506–8521.
- [19] Nguyen T.T.V., Xie X., Xu J., Wu Y., Hong M., Liu X. Plasmonic bimetallic nanodisk arrays for DNA conformation sensing. *Nanoscale*, 2019, **11** (41), P. 19291–19296.
- [20] Szunerits S., Saada H., Pagneux Q., Boukherroub R. Plasmonic Approaches for the Detection of SARS-CoV-2 Viral Particles. *Biosensors*, 2022, **12** (7), 548.
- [21] Liu C.H., Hong M.H., Cheung H.W., Zhang F., Huang Z.Q., Tan L.S., Hor T.S. A. Bimetallic structure fabricated by laser interference lithography for tuning surface plasmon resonance. *Optics Express*, 2008, **16** (14), P. 10701–10709.
- [22] Xu L., Tan L.S., Hong M.H. Tuning of localized surface plasmon resonance of well-ordered Ag/Au bimetallic nanodot arrays by laser interference lithography and thermal annealing. *Applied Optics*, 2011, **50** (31), P. 74–79.
- [23] Nguyen T.T.V. Development of plasmonic nanostructures for biological sensing. Ph.D dissertation, National University of Singapore, 2013.
- [24] Tombelli S., Minunni M., Mascini M. Analytical applications of aptamers. *Biosensors and Bioelectronics*, 2005, **20** (12), P. 2424–2434.
- [25] Zhou J., Rossi J. Aptamers as targeted therapeutics: current potential and challenges. *Nature Reviews Drug Discovery*, 2017, **16** (3), P. 181–202.
- [26] Taghdisi S.M., Danesh N.M., Lavaee P., Sarreshtehdar Emrani A., Ramezani M., Abnous K. Aptamer Biosensor for Selective and Rapid Determination of Insulin. *Analytical Letters*, 2015, **48** (4), P. 672–681.
- [27] Connor A.C., Frederick K.A., Morgan E.J., McGown L.B. Insulin Capture by an Insulin-Linked Polymorphic Region G-Quadruplex DNA Oligonucleotide. *J. of the American Chemical Society*, 2006, **128** (15), P. 4986–4991.
- [28] Zhang X., Zhu S., Deng C., Zhang X. An aptamer based on-plate microarray for high-throughput insulin detection by MALDI-TOF MS. *Chemical Communications*, 2012, **48** (21), P. 2689–2691.
- [29] Malik R., Roy I. Stabilization of bovine insulin against agitation-induced aggregation using RNA aptamers. *Int. J. of Pharmaceutics*, 2013, **452** (1), P. 257–265.
- [30] Wu Y., Midinov B., White R.J. Electrochemical Aptamer-Based Sensor for Real-Time Monitoring of Insulin. *ACS Sensors*, 2019, **4** (2), P. 498–503.
- [31] Taib M., Tan L.L., Abd Karim N.H., Ta G.C., Heng L.Y., Khalid B. Reflectance aptasensor based on metal salphen label for rapid and facile determination of insulin. *Talanta*, 2020, **207**, 120321.
- [32] Willets K.A., Duyne R.P.V. Localized Surface Plasmon Resonance Spectroscopy and Sensing. *Annual Review of Physical Chemistry*, 2007, **58** (1), P. 267–297.
- [33] Grabar K.C., Freeman R.G., Hommer M.B., Natan M.J. Preparation and Characterization of Au Colloid Monolayers. *Analytical Chemistry*, 1995, **67** (4), P. 735–743.
- [34] Liu J., Cao Z., Lu Y. Functional Nucleic Acid Sensors. *Chemical Reviews*, 2009, **109** (5), P. 1948–1998.
- [35] Shrivastava A. Methods for the determination of limit of detection and limit of quantitation of the analytical methods. *Chronicles of Young Scientists*, 2011, **2**, P. 21–25.

---

Submitted 27 November 2023; revised 6 March 2024; accepted 10 March 2024

#### Information about the authors:

Thanh Thi Van Nguyen – School of Materials Science and Engineering, Hanoi University of Science and Technology, No.1 Dai Co Viet street, Hanoi 100000, Vietnam; ORCID 0009-0005-2040-2781; thanh.nguyenthivan@hust.edu.vn